Nuclear Moments and Deformation Change in $^{184}Au^{g,m}$ from Laser Spectroscopy

F. Le Blanc, J. Obert, J. Oms, J. C. Putaux, B. Roussière, and J. Sauvage
Institut de Physique Nucléaire, IN2P3-CNRS, 91406 Orsay Cedex, France

J. Pinard, L. Cabaret, and H. T. Duong
Laboratoire Aimé Cotton, 91405 Orsay Cedex, France

G. Huber, M. Krieg, and V. Sebastian
Institut für Physik der Universität Mainz, 55099 Mainz, Germany

J. Crawford and J. K. P. Lee
Foster Radiation Laboratory, McGill University, H3A2B1 Montréal, Canada

J. Genevey and F. Ibrahim
Institut des Sciences Nucléaires, IN2P3-CNRS, 38026 Grenoble Cedex, France

and ISOLDE Collaboration
CERN, 1211 Geneva 23, Switzerland

(Received 21 April 1997)

Resonance ionization spectroscopy (RIS) was performed on desorbed Au, and the complete hyperfine spectrum of both isomeric and ground states of the short lived ^{184}Au nucleus has been recorded from the $5d^{10}6s\,^2S_{1/2} \rightarrow 5d^{10}6p\,^2P_{3/2}$ optical transition. The nuclear moments of both states and the mean square charge radius changes were measured. The magnetic moments were determined to be $\mu_{I=5}^{184g} = +2.07(2)\mu_N$ and $\mu_{I=2}^{184m} = +1.44(2)\mu_N$ and the spectroscopic quadrupole moments to be $Q_s^{184g} = +4.65(26)b$ and $Q_s^{184m} = +1.90(16)$ b. A difference in the mean square charge radius $\delta\langle r_c^2\rangle^{184g,184m} = -0.036(3)$ fm^2 was found. [S0031-9007(97)03992-6]

PACS numbers: 21.10.Ky, 21.10.Ft, 42.62.Fi

Light gold isotopes belong to a mass region where drastic changes in the nuclear charge radius have been measured by laser spectroscopy. Such alterations have shown alternating shape transitions and deformation changes between neighboring isotopes. This was observed in mercury [1,2], gold [3–5], and to a lesser degree in platinum isotopes [6,7]. Different deformations have also been observed in the states of the same nucleus. The best example is ^{185}Hg where the large radius difference measured between its ground and isomeric state [8] has shown a prolate-oblate shape coexistence which was confirmed later from γ-ray spectroscopic studies [9,10].

In this context, the doubly odd nucleus ^{184}Au with its isomeric state at 68 keV excitation energy [11,12] is particularly interesting to investigate since it is located in the middle of this transitional region [13,14]: States corresponding to prolate and oblate or triaxial shapes coexist in ^{183,185}Au [9,15,16] and ^{185}Hg, while ^{183}Pt is prolate in all its low energy states [17–19]. Several nuclear spectroscopy studies were performed on ^{184}Au, and it has been established that (i) a shape coexistence is excluded at low excitation energy [20], and (ii) the spin and parity are 5^+ for the ground state and 2^+ for the isomer with the following proton-neutron ($\pi \otimes \nu$) configurations: $\pi h\frac{9}{2} \otimes \nu\frac{7}{2}[514]$ and $\pi h\frac{9}{2} \otimes \nu\frac{1}{2}[521]$, respectively [21]. Furthermore, calculations using rotor + one-quasiparticle and rotor + two-quasiparticle coupling models were performed on the $N = 105$ isotones ^{183}Pt, ^{182}Ir [22], ^{185}Hg, and ^{184}Au [23]. They show that the relative energy location of the 5^+ and 2^+ states suggests a deformation change, either between $^{184}Au^g$ and $^{184}Au^m$ or between ^{184}Au and its neighboring isotopes. Therefore, the determination of the quadrupole moment in both isomer and ground states, as well as the change in the mean square charge radius between them, is crucial to fully characterize their nuclear shape. Moreover, a measurement of the magnetic moments of the two states will allow a clear confirmation of the $\pi \otimes \nu$ configurations. In addition, the $\pi \otimes \nu$ coupling scheme can be defined from the quadrupole moment values.

In this Letter, we present optical measurements on ^{184}Au. The hyperfine structure is measured providing the magnetic A and electrostatic B hyperfine constants of the levels involved in the atomic transition as well as the isomeric shift. A is related to the magnetic moment μ_I, and B to the spectroscopic quadrupole moment Q_s. The isomeric shift, which is the displacement of the centers of gravity of the two hyperfine spectra, determines the mean square charge radius variation $\delta\langle r_c^2\rangle^{184g,184m}$. These measurements are particularly challenging since gold beams are no longer available from

isotope separators and the half-lives of both states are relatively short ($T_{1/2,m} \sim 45$ s and $T_{1/2,g} \sim 20$ s [12,24] or $T_{1/2,m} = 28$ s and $T_{1/2,g} = 12$ s [25]). We developed the COMPLIS experimental setup [26] which consists of laser desorbing implanted atoms followed by a RIS (resonance ionization spectroscopy) study.

The radioactive mercury isotopes are produced via $(p, 3pxn)$ reactions on the ISOLDE lead target [27] with the 1 GeV CERN PS-booster proton beam. The ions are extracted at 60 kV and mass separated by the high resolution separator (HRS) of ISOLDE. They enter the COMPLIS beam line, are slowed to 1 kV, and are thus deposited on the first atomic layers of a rotating graphite substrate. Then, the daughter gold atoms obtained via β^+/EC decay are desorbed by a Nd:YAG laser and selectively ionized by a set of two pulsed, tunable dye lasers. The use of pulsed laser desorption to generate a pulsed atomic beam synchronized to the ionizing laser pulses results in a large increase in sensitivity over RIS on continuous atomic beams. The desorption laser is focused to a vertical line of 2 mm by 0.02 mm and fired at a repetition rate of 10 Hz. The first excitation step at 243 nm ($5d^{10}6s^2S_{1/2} \rightarrow 5d^{10}6p^2P_{3/2}$), which yields the spectroscopic information, is produced using an argon ion-pumped single-mode tunable dye laser. High resolution may be achieved by injection locking a pulsed dye laser to the frequency of the cw laser. This is done by adding a YAG-pumped dye cell to the cavity of a tunable cw dye laser [28]. The pulses delivered by this system are frequency tripled in order to obtain the 243 nm UV wavelength. The ionization step at 300 nm is obtained by a frequency doubled commercial dye laser pumped by the same Nd:YAG laser. The resulting gold ions are accelerated to 59 kV and magnetically separated from the light masses desorbed as ions. Finally, they are detected by microchannel plates and mass identified by time of flight. The frequency scan over the hyperfine structures of both isomer and ground state is carried out as follows: The Hg ions are collected during 19.2 or 38.4 s. The desorption of the gold atoms is then made over the entire collection spot on the slowly rotating target at a given frequency step. After the desorption is complete, a new cycle of implantation desorption is run at an advanced frequency step (from 60 to 220 MHz further depending on the resolution required). Whenever the laser frequency corresponds to a hyperfine transition, the desorbed atoms are excited and ionized by the other fixed laser frequency. The number of counted ions at the detector is directly proportional to the intensity of the hyperfine transition. The motion of the target, the firing of the laser, the frequency scan, and the data acquisition are controlled by a multitask SUN workstation. The desorption parameters (choice of the graphite target, power, and focusing of the laser, etc.) and the ionization parameters were optimized with the use of a stable gold-beam injector linked to the COMPLIS incident beam line. With this apparatus, the efficiency was measured of about 10^{-5} with a resolution of 300 MHz.

The measured hyperfine spectrum of $^{184}Au^{g+m}$ is shown in Fig. 1. Two widely spread groups can be identified each with hyperfine lines clearly resolved. In order to distinguish the lines corresponding to the isomer

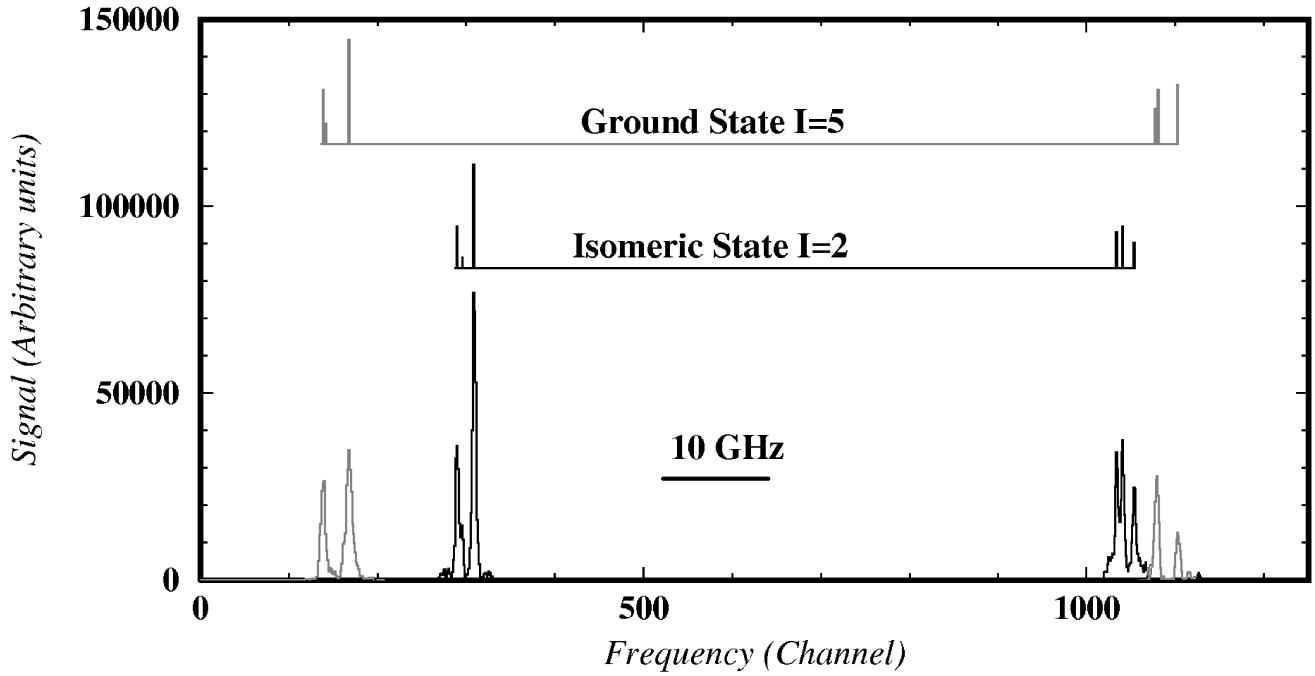

FIG. 1. Hyperfine spectrum of $^{184}Au^{g+m}$ (the ground state lines have been magnified by a factor of 5). The two spectra above the experimental one have been calculated with the extracted hyperfine constants A and B and the isomeric shift $\Delta\nu$.

TABLE I. Isotope shift and mean square charge radius variation in ^{184}Au. ^{197}Au is taken as the reference isotope. The value of $|\langle\beta^2\rangle^{1/2}|$ (^{197}Au) = 0.113 is taken from the calculation of Möller and Nix [34].

A	I	$\delta\nu^{197,A}$ (GHz)	$\lambda^{197,A}$ (fm^2)	$\delta\langle r_c^2\rangle^{197,A}$ (fm^2)	$\delta\langle\beta^2\rangle^{197,A}$	$\lvert\langle\beta^2\rangle^{1/2}\rvert$
184^g	5	2.81(30)	−0.073(12)	−0.064(12)	0.0524(11)	0.255(3)
184^m	2	4.20(30)	−0.106(12)	−0.100(12)	0.0493(11)	0.249(3)

from those connected to the ground state, we have compared the hyperfine spectra obtained using 19.2 and 38.4 s as collection time. Under these conditions, it can be established from the ^{184}Au level scheme, obtained from the β decay of ^{184}Hg [21,29], that the ratio between the number of gold nuclei in its isomeric state and its ground state varies from 45 (for 19.2 s) to 22 (for 38.4 s). The ground state hyperfine spectrum can thus be clearly identified with two less intense groups of lines compared to those of the isomer. For each state, the six lines were fitted leading to the A hyperfine constant for the $^2S_{1/2}$ atomic ground state and $^2P_{3/2}$ excited state and the B hyperfine constant for the $^2P_{3/2}$ state as well as the isomeric shift in the optical transition. We also simultaneously recorded the hyperfine spectrum of the stable gold isotope in order to obtain the absolute position of the centers of gravity. The relative frequency calibration was obtained by a Fabry-Pérot etalon.

The measured isotope shift $\delta\nu^{A,A'}$ between two isotopes of mass A and A' can be written as the sum of the field shift $\delta\nu_{FS}^{A,A'}$ and the mass shift $\delta\nu_{MS}^{A,A'}$ [30]. For the 243 nm line in Au, $\delta\nu_{MS}^{197,184} = -0.31(22)$ GHz is deduced from Ref. [31]. The field shift is related to the change in the nuclear charge distribution via $\delta\nu_{FS}^{A,A'} = F_i \cdot \lambda^{A,A'}$, where $\lambda^{A,A'}$ is a nuclear quantity related to the change in the nuclear charge radius [30]. The electronic factor F_{243} is obtained by a relativistic multiconfiguration Dirac-Fock (MCDF) calculation [32]: $F_{243} = -42.73$ GHz/fm^2. From the measured isomeric shift in ^{184}Au $\delta\nu^{184g,184m} = 1.39(10)$ GHz,

$$\delta\langle r_c^2\rangle^{184g,184m} = -0.036(3)\ \text{fm}^2.$$

The mean square deformation variation $\delta\langle\beta^2\rangle$ can be extracted via

$$\delta\langle r^2\rangle^{A,A'} = \delta\langle r^2\rangle_{\text{sph}}^{A,A'} + \frac{5}{4\pi}\langle r^2\rangle_{\text{sph}}\delta\langle\beta^2\rangle^{A,A'},$$

where $\delta\langle r^2\rangle_{\text{sph}}$ and $\langle r^2\rangle_{\text{sph}}$ are calculated according to the prescription of Myers and Schmidt [33]. This leads to $\delta\langle\beta^2\rangle^{184g,184m} = -0.0031(2)$. Table I and Fig. 2 show the mean square charge radius variation of ^{184}Au^{g+m} and other gold isotopes [3,4,35]. The value of $\delta\langle r_c^2\rangle^{197,184}$ measured by Krönert *et al.* [35] is consistent with ours for $I = 2$. The spin was not yet known and thus they report values from $\delta\langle r_c^2\rangle^{197,184} = -0.137$ fm^2 for $I = 3$ to -0.22 fm^2 for high spin values. Since our experiment and theirs used the same type of pulsed laser ion source made from the decay of mercury isotopes, they could not have measured the $I = 5$ ground state without having identified the isomeric state which is fed by almost all of the radioactive decay.

For ^{197}Au, the spectroscopic quadrupole moment $Q_s = 0.547(16)$ b has been measured from a muonic x-ray experiment [36]. We measured for this isotope $B(^2P_{3/2}) = +0.336(10)$ GHz which is in agreement with the B factor measured by Goldman *et al.* [37], $|B(^2P_{3/2})| = 0.328(2)$ GHz. With the measurement of $B(^2P_{3/2})$ in ^{184}Au we determined the Q_s values using

$$Q_s(^x\text{Au}) = \frac{B(^x\text{Au})}{B(^{197}\text{Au})}\,Q_s(^{197}\text{Au})$$

and the $B(^{197}\text{Au})$ from Ref. [37]. No Sternheimer correction is needed due to the use of muonic data. To extract the intrinsic quadrupole moment which gives the sign of the nuclear deformation, one has to know K, the projection of the spin I on the symmetry axis; the Q_0 and β values (see Table II) have been deduced assuming axial symmetry with $K = I$. Concerning the isomer, we observed a small difference between the rms deformation value extracted from $\delta\langle r_c^2\rangle$ and the deformation extracted from Q_s (see Table II). This can be explained by a small admixture of $K = 1$ (∼8%) and $K = 2$ components in the isomeric wave function. Concerning the ground state, $\langle\beta^2\rangle^{1/2}$ and β are so close that a pure value of $K = 5$ can be deduced.

The magnetic moments were extracted from the measured $A(^2S_{1/2})$ for both ground state and isomer using the equation from Ref. [3],

$$\mu_I = A(^2S_{1/2})\,(I/29.005)\mu_N\,,$$

and neglecting the hyperfine anomaly with respect to experimental uncertainties. The μ_I obtained for the isomer

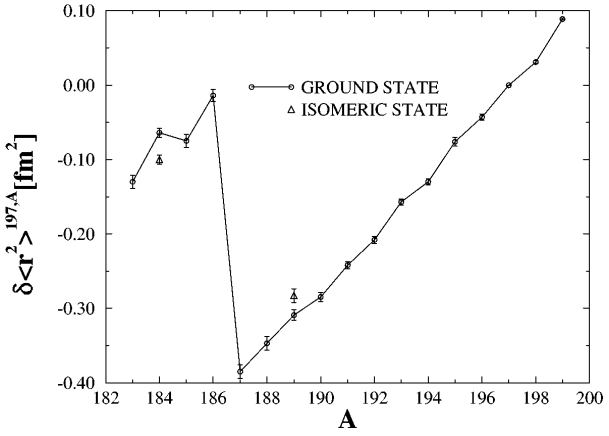

FIG. 2. Mean square charge radius variation measured in the gold isotopes (this work and Refs. [3,4,35]).

TABLE II. Hyperfine constants and nuclear moments in ^{184}Au. The deformation parameter extracted from the quadrupole moment is compared to the rms deformation parameter extracted from the $\delta\langle r_c^2\rangle$.

A	I	$A(^2S_{1/2})$ (GHz)	$A(^2P_{3/2})$ (GHz)	$B(^2P_{3/2})$ (GHz)	μ_I (μ_N)	Q_s (b)	K	Q_0 (b)	β	$\lvert\langle\beta^2\rangle^{1/2}\rvert$
184^g	5	11.99(11)	0.053(12)	2.79(13)	+2.07(2)	+4.65(26)	5	+8.06(45)	+0.264(14)	0.255(3)
184^m	2	20.92(24)	0.096(20)	1.14(9)	+1.44(2)	+1.90(16)	2	+6.65(56)	+0.221(17)	0.249(3)

(see Table II) is in perfect agreement with that measured by Krönert *et al.* [35], which is $\mu_I^{184} = 1.450(15)\mu_N$ for an $I = 2$ spin value, and consistent with that of Ref. [24], which is $\mu_I^{184} = 1.30(28)\mu_N$. Since the 5^+ and 2^+ states have almost pure $K = 5$ and $K = 2$ wave functions, they correspond very likely to the $\pi\frac{3}{2}[532] \otimes \nu\frac{7}{2}[514]$ and the $\pi\frac{3}{2}[532] \otimes \nu\frac{1}{2}[521]$ configurations, respectively. It is worth noting that the $h_{9/2}$ proton, decoupled from the core by the Coriolis force in ^{183,185}Au [9,15], becomes the $3/2^-[532]$ proton ($h_{9/2}$ parentage) that is strongly coupled in ^{184}Au. The magnetic moments may thus be estimated following the method given by Ekström *et al.* [38]:

$$\mu = \frac{K}{I+1}\left(g_{K_p}K_p + g_{K_n}K_n + g_R\right).$$

The g_{K_p} and g_{K_n} factors were extracted from the magnetic moments in the neighboring isotopes calculated as described in Ref. [39] but using a ^{186}Hg core constrained to the β deformation close to that extracted from the $\delta\langle r_c^2\rangle$ measurements. For the isomer, we found $\mu_I^{184m} = 1.2\mu_N$ for $g_{s\text{free}}$ and $\mu_I^{184m} = 1.4\mu_N$ for $0.6g_{s\text{free}}$, which are in agreement with the experimental value $\mu_{I\text{exp}}^{184m} = 1.44(2)\mu_N$. For the ground state, we found $\mu_I^{184g} = 2.3\mu_N$ for $g_{s\text{free}}$ and $\mu_I^{184g} = 2.2\mu_N$ for $0.6g_{s\text{free}}$ to be compared with $\mu_{I\text{exp}}^{184g} = 2.07(2)\mu_N$: The agreement is also good. The experimental results are thus fairly well reproduced by these calculations which strongly support the proposed configurations for both states. Figure 2 shows that the deformation of ^{184}Au^m is similar to that expected from measurements in ^{183,185}Au, while ^{184}Au^g is slightly more deformed. However, more measurements on the neighboring isotones are crucial in order to place the interpretation of the state inversion in ^{184}Au as due to a deformation change on a strong basis. ^{183}Pt is a perfect candidate since the same neutron configurations are involved in both ground and isomeric states.

We wish to thank M. Ducourtieux, A. Ferro, and J.C. Potier for experimental help, as well as N. Barré and C. Véron for the conception of the acquisition system.

[1] J. Bonn *et al.*, Phys. Lett. **38B**, 308 (1972).
[2] G. Ulm *et al.*, Z. Phys. A **325**, 247 (1986).
[3] K. Wallmeroth *et al.*, Nucl. Phys. **A493**, 224 (1989).
[4] G. Savard *et al.*, Nucl. Phys. **A512**, 241 (1990).
[5] G. Passler *et al.*, Nucl. Phys. **A580**, 173 (1994).
[6] H.T. Duong *et al.*, Phys. Lett. B **217**, 401 (1989).
[7] T. Hilberath *et al.*, Z. Phys. A **342**, 1 (1992).
[8] P. Dabkiewicz *et al.*, Phys. Lett. **82B**, 199 (1979).
[9] C. Bourgeois *et al.*, Nucl. Phys. **A386**, 308 (1982), and references therein.
[10] F. Hannachi *et al.*, Z. Phys. A **330**, 15 (1988).
[11] R. Eder *et al.*, Hyperfine Interact. **60**, 83 (1990).
[12] K. Zaerpoor *et al.*, Phys. Rev. C **55**, 2697 (1997).
[13] K. Heyde *et al.*, Phys. Rep. **102**, 291 (1983).
[14] J.L. Wood *et al.*, Phys. Rep. **215**, 101 (1992).
[15] M.I. Macias-Marques *et al.*, Nucl. Phys. **A427**, 205 (1984).
[16] M.O. Kortelahti *et al.*, J. Phys. G **14**, 1361 (1988).
[17] A. Visvanathan *et al.*, Phys. Rev. C **19**, 282 (1979).
[18] B. Roussière *et al.*, Nucl. Phys. **A504**, 511 (1989).
[19] J. Nyberg *et al.*, Nucl. Phys. **A511**, 92 (1990).
[20] F. Ibrahim *et al.*, Phys. Rev. C **53**, 1547 (1996).
[21] F. Ibrahim *et al.*, Z. Phys. A **350**, 9 (1994).
[22] J. Sauvage *et al.*, Nucl. Phys. **A592**, 221 (1995).
[23] F. Ibrahim *et al.*, in *Proceedings of the Exotic Nuclei and Atomic Masses Conference, Arles, France, 1995*, edited by M. de Saint Simon and O. Sorlin (Editions Frontières, Gif-sur-Yvette, 1995), p. 493.
[24] I. Romanski *et al.*, Hyperfine Interact. **75**, 457 (1992).
[25] A. Knipper (private communication).
[26] F. Le Blanc *et al.*, in *Proceedings of the 8th International Symposium on Capture Gamma-Ray Spectroscopy and Related Topics, Fribourg, Switzerland, 1993*, edited by J. Kern (World Scientific, Singapore, 1994), p. 1001.
[27] J. Lettry *et al.*, in *Joint Proceedings of the 13th Meeting of the International Collaboration on Advanced Neutron Sources, PSI-Proc. 95-02, ICANS-XIII*, edited by G.S. Bauer and R. Bercher (Villigen, Switzerland, 1995), p. 595.
[28] J. Pinard and S. Liberman, Opt. Commun. **20**, 344 (1977).
[29] B. Roussière *et al.*, in *Proceedings of the 8th International Symposium on Capture Gamma-Ray Spectroscopy and Related Topics, Fribourg, Switzerland, 1993*, edited by J. Kern (World Scientific, Singapore, 1994), p. 231.
[30] E.C. Seltzer, Phys. Rev. **188**, 1916 (1969).
[31] K. Heilig and A. Steudel, At. Data Nucl. Data Tables **14**, 613 (1974).
[32] A. Rosen, B. Fricke, and G. Torbohm, Z. Phys. A **316**, 157 (1984).
[33] W.D. Myers and K.H. Schmidt, Nucl. Phys. **A410**, 61 (1983).
[34] P. Möller and J.R. Nix, At. Data Nucl. Data Tables **26**, 165 (1981).
[35] U. Krönert *et al.*, Z. Phys. A **331**, 521 (1988).
[36] R.J. Powers *et al.*, Nucl. Phys. **A230**, 413 (1974).
[37] G. Goldmann, C. Hahn, and J. Ney, Z. Phys. **225**, 1 (1969).
[38] C. Ekström, H. Rubinsztein, and P. Möller, Phys. Scr. **14**, 199 (1976).
[39] M.G. Porquet *et al.*, Nucl. Phys. **A451**, 365 (1986).